Involvement of Glycine 141 in Substrate Activation by Enoyl-CoA Hydratase†

Alasdair F. Bell,‡ Jiaquan Wu,‡ Yuguo Feng,‡ and Peter J. Tonge*,‡,§

Department of Chemistry and Graduate Programs in Biophysics and in Molecular and Cellular Biochemistry, State University of New York at Stony Brook, Stony Brook, New York 11794-3400

Received July 25, 2000; Revised Manuscript Received November 1, 2000

ABSTRACT: Raman spectroscopy has been used to investigate the structure of a substrate analogue, hexadienoyl-CoA (HD-CoA), bound to wild-type enoyl-CoA hydratase and G141P, a mutant in which a hydrogen bond to the substrate carbonyl has been removed. Raman spectra of isotopically labeled HD-CoAs, together with normal mode calculations, confirm the selective ground-state polarization of the enone fragment previously suggested to occur on binding to the wild-type enzyme [Tonge, P. J., Anderson, V. E., Fausto, R., Kim, M., Pusztai-Carey, M., and Carey, P. R. (1995) *Biospectroscopy 1*, 387−394]. In addition, Raman spectra of HD-CoA bound to the G141P mutant enzyme demonstrate that the hydrogen bond between the G141 amide NH group and the substrate carbonyl is critical for polarization and activity. Replacement of G141 with proline results in an approximately 10^6-fold decrease in k_{cat} and eliminates the ability of the enzyme to polarize the substrate analogue. As G141 is part of a consensus sequence in the enoyl-CoA hydratase superfamily, the results presented here provide direct evidence for the importance of the oxyanion hole in the reactions catalyzed by other family members.

Enoyl-CoA hydratase (EC 4.2.1.17) catalyzes the hydration of *trans*-2-enoyl-CoA thiolesters to the corresponding 3(*S*)-hydroxyacyl-CoA compounds (Figure 1) (*2*). The reaction is the second step in the fatty acid β-oxidation pathway that results in the sequential shortening of fatty acids by two carbon units. The mammalian short-chain enzyme is most active with C4−C8 fatty acids (*3*), and the reaction of *trans*-2-crotonyl-CoA (*trans*-2-butenoyl-CoA) proceeds close to the diffusion-controlled rate for encounter of substrate and enzyme with $V/K > 5 \times 10^8$ M^{-1} s^{-1} (*4*). Our current research focuses on dissecting the factors that contribute to the catalytic power of the enzyme. Using Raman spectroscopy, information is provided on changes in the ground-state structure of the substrate upon binding to the enzyme and on interactions between enzyme and substrate that are expected to strengthen in the transition state as charge reorganization occurs during the reaction. Coupling the Raman studies with site-directed mutagenesis enables us to probe the importance of specific enzyme−substrate contacts. When combined with reactivity measurements, this approach provides a direct structure−reactivity correlation for the enzyme-catalyzed reaction.

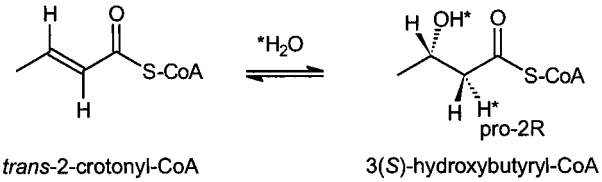

FIGURE 1: Reaction catalyzed by enoyl-CoA hydratase.

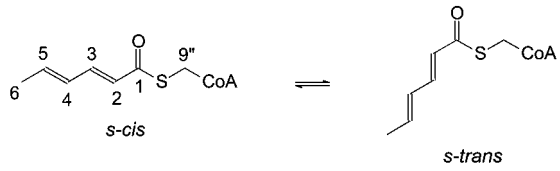

FIGURE 2: Structure and numbering scheme for *s-cis* and *s-trans* conformers of hexadienoyl-CoA. Position 9″ is the terminal methylene group in the pantetheine portion of CoA (*7*).

Hexadienoyl-CoA (HD-CoA; Figure 2) and cinnamoyl-CoA have previously been used in difference Raman spectroscopic investigations of substrate analogues binding to enoyl-CoA hydratase (*1*, *5*). The additional conjugation in these compounds, resulting from a second double bond (HD-CoA) or phenyl ring (cinnamoyl-CoA), shifts the thermodynamic balance for the reaction in favor of the unsaturated substrate (*6*). Consequently, whereas the equilibrium for the hydration of crotonyl-CoA lies 7.5:1 in favor of the product, the substrate analogues are not detectably hydrated by the enzyme. The previous Raman studies reached two main conclusions: first, that the π-electrons of the enone fragment of HD-CoA were selectively polarized by the enzyme and, second, on the basis of low-temperature studies, that the enzyme bound the *s-cis* conformer around the C1−C2 single bond of the dienone. Subsequently, sequence homology−modeling based on the X-ray structure of 4-chlorobenzoyl-CoA dehalogenase resulted in the prediction,

† This work was supported by NSF Grant MCB9604254, NIH Grant AI40982, U.S. Army Research Office Grant DAAG559710083 to P.J.T., and an American Heart Association Postdoctoral Fellowship 0020191T to A.F.B. MALDI-MS data were collected at the Center for Analysis and Synthesis of Macromolecules, SUNY, Stony Brook, supported by NIH Grant RR02427, and the Center for Biotechnology. The NMR facility at SUNY, Stony Brook, is supported by grants from the NSF (CHE9413510) and the NIH (1S10RR554701). The departmental centrifuge facility is supported by NSF Grant CHE9808439.

* To whom correspondence should be addressed at the Department of Chemistry. Telephone: (631) 632 7907. Fax: (631) 632 5797. E-mail: peter.tonge@sunysb.edu.

‡ Department of Chemistry.

§ Graduate Programs in Biophysics and in Molecular and Cellular Biochemistry.

10.1021/bi001733z CCC: $20.00
Published on Web 01/20/2001

substantiated by site-directed mutagenesis, of two catalytic glutamate residues in the enoyl-CoA hydratase active site (E144 and E164) (*4*, *7*, *8*). In addition, the modeling studies, together with X-ray crystallographic studies (*9*, *10*), indicated the presence of an oxyanion hole in which the enzyme donates two hydrogen bonds to the substrate carbonyl, from the backbone NH groups of G141 and A98. G141 is part of a consensus sequence in the enoyl-CoA hydratase superfamily (*11*), and the crystal structure of 4-chlorobenzoyl-CoA dehalogenase with product bound indicates that G114, the G141 homologue, also hydrogen bonds to the substrate carbonyl (*12*). Structures for two other family members, dienoyl-CoA isomerase (*13*) and methylmalonyl-CoA decarboxylase (*14*), have resulted in proposals that G143 (isomerase) and G110 (decarboxylase) also contribute to oxyanion holes in these enzymes. Additionally, in each case the conserved glycine lies at the N-terminus of an α-helix, raising the possibility that the helix dipole is also involved in stabilizing charge accumulation on the substrate carbonyl (*7*, *9*, *11*, *13*−*17*).

The current difference Raman study builds upon previous Raman experiments (*1*, *5*). The discussion of the results is split into two sections. First, new isotope-labeled Raman data, together with normal mode calculations, are used to refine the assignments of the double bond stretching bands that appear between 1500 and 1700 cm^{-1} and to extend these assignments to the C−C single bond stretching modes. These data confirm the selective ground-state electron polarization of the enone fragment in HD-CoA and provide a physical explanation for the observed vibrational data. Second, we compare the Raman spectra of HD-CoA bound to the mutant G141P with that of wild-type enoyl-CoA hydratase. Although the G to P substitution is not a conservative replacement, the Ramachandran angles of G141 (ϕ −54° and ψ −31°) are compatible with substitution by a proline [preferred ϕ −60° (*18*)]. In addition, proline is a good helix-capping residue (*19*), and analysis of the G141P enzyme indicates that the active site is intact. Consequently, the loss of polarization we observe for HD-CoA bound to the mutant implicates the G141 hydrogen bond as an important component of substrate polarization, consistent with the approximately 10^6-fold decrease in activity we observe for this mutant.

EXPERIMENTAL PROCEDURES

Chemicals. Hexadienoic acid, 1,1′-carbonyldiimidazole, acetaldehyde, [1-^{13}C]acetyl chloride, and coenzyme A (lithium salt; CoA)[1] were purchased from Sigma Chemical Co. [1,3-$^{13}C_2$]Malonic acid (99% ^{13}C), [2-^{13}C]malonic acid (99% ^{13}C), and $H_2{}^{18}O$ (95−98% ^{18}O) were purchased from Cambridge Isotope Labs.

Hexadienoyl-CoA. Hexadienoyl-CoA (HD-CoA) was synthesized from hexadienoylimidazole and CoA essentially as described (*1*). Briefly, 30 mg (0.039 mmol) of CoA (lithium salt) was dissolved in 1 mL of 0.1 M $NaHCO_3$ and reacted at room temperature with 10 mg (0.062 mmol) of hexadienoylimidazole dissolved in 1 mL of acetonitrile. The reaction progress was monitored by following the free thiol concentration of CoA using 5,5′-dithiobis(2-nitrobenzoic acid) (DTNB) (*20*). When no free thiol was detected, the organic solvent was removed in vacuo, and HD-CoA was purified by HPLC (Shimadzu) using an Alltech Econosil C18 semipreparative column. HPLC was performed at a flow rate of 4 mL/min using 20 mM ammonium acetate/1.75% acetonitrile as buffer A and running a 0−75% gradient of acetonitrile in 60 min. Elution was monitored at 260 and 290 nm using a Shimadzu SPD-10A UV−vis detector. The fractions with an A_{260}/A_{290} ratio of 1.1 were pooled and lyophilized. To remove ammonium acetate, a second lyophilization from water was performed. ^{1}H NMR (600 MHz, D_2O): δ 0.78 (s, 3H, 11′ CH3), 0.91 (s, 3H, 10′ CH3), 1.84 (d, 3H, CH3hd), 2.44 (t, 2H, H6″), 3.05 (t, 2H, H9″), 3.37 (t, 2H, H8″), 3.46 (t, 2H, H5″), 3.58 (q, 1H, H1″B), 3.86 (q, 1H, H1″A), 4.04 (s, 1H, H3″), 4.25 (s, 2H, H5′), 4.60 (s, 1H, H4′), 6.08 (d, 1H, H2hd), 6.15 (d, 1H, H1′), 6.18 (m, 1H, H4hd), 6.32 (m, 1H, H5hd), 7.14 (m, 1H, H3hd), 8.24 (s, 1H, H2), 8.54 (s, 1H, H8). The CoA H2′ and H3′ resonances are obscured by the solvent resonance. ^{13}C NMR (75 MHz, D_2O): δ 21.13 (C11″ + C6hd), 23.74 (C10″), 30.76 (C9″), 38.30 (C6″), 41.15 (C2″), 41.26 (C5″), 41.60 (C8″), 68.44 (C5′), 74.71 (C1″), 76.79 (C2′), 77.03 (C3′ + C3″), 86.64 (C4′), 89.34 (C1′), 121.51 (C5), 127.81 (C5hd), 131.98 (C4hd), 142.68 (C8), 145.91 (C2hd), 146.74 (C3hd), 152.18 (C4), 155.72 (C2), 158.46 (C6), 176.87 (C7″), 177.61 (C4″), 196.52 (C1hd). Molecular weight: ESI-MS $[M - H]^-$ calculated for $[C_{27}H_{41}N_7O_{17}P_3S] = 860.15$, found = 860.4.

^{18}O-HD-CoA. Hexadienoyl-CoA labeled with ^{18}O in the carbonyl oxygen (^{18}O-HD-CoA) was synthesized essentially as described previously (*1*), except that oxalyl chloride was used in place of thionyl chloride. The ^{18}O label was introduced into the carbonyl group of hexadienoic acid by formation of hexadienoyl chloride followed by hydrolysis with $H_2{}^{18}O$. Following 10 cycles of acid chloride formation and hydrolysis, the resulting [^{18}O]hexadienoic acid was converted to the CoA derivative by the procedure described above. ^{1}H NMR chemical shifts were identical to those given above for unlabeled HD-CoA. Molecular weight: ESI-MS $[M - H]^-$calculated for $[C_{27}H_{41}N_7O_{16}{}^{18}OP_3S] = 862.15$, found = 862.4. ESI-MS analysis gave 93.7% ^{18}O labeling.

2-^{13}C-HD-CoA. Hexadienoyl-CoA labeled with ^{13}C in the hexadienoyl C2 position (2-^{13}C-HD-CoA) was synthesized as follows using a modification of the procedure described by Koo et al. (*21*). Thus, 0.2 mL (2.5 mmol) of freshly distilled crotonaldehyde was added dropwise to a solution of 100 mg (0.94 mmol) of [2-^{13}C]malonic acid in 0.25 mL of freshly distilled pyridine at 80 °C. After refluxing at 120 °C for 4 h, the reaction mixture was added to about 1 mL of H_2O and acidified to pH 1.5 with concentrated sulfuric acid. [2-^{13}C]Hexadienoic acid was extracted from the resulting solution with diethyl ether and subsequently activated and coupled with CoA as described above. ^{1}H NMR chemical shifts and coupling constants were identical to those observed for unlabeled HD-CoA except that the doublet at 6.08 ppm, assigned to the proton attached to the hexadienoyl C2 carbon, was split into two doublets at 5.95 and 6.21 ppm ($^1J_{H-C}$ = 156 Hz). The ^{13}C NMR spectrum was identical to that of the unlabeled HD-CoA, except that the peak at 145.91 ppm was greatly increased in intensity, consistent with ^{13}C labeling at C2.

[1] Abbreviations: CoA, coenzyme A (lithium salt); HD-CoA, *trans,trans*-2,4-hexadienoyl-CoA; DTNB, 5,5′-dithiobis(2-nitrobenzoic acid); DAC-CoA, (dimethylamino)cinnamoyl-CoA; ITC, isothermal titration calorimetry.

3-^{13}C-HD-CoA. Hexadienoyl-CoA labeled with ^{13}C in the hexadienoyl C3 position (3-^{13}C-HD-CoA) was synthesized as follows. Initially, [1-^{13}C]crotonic acid was synthesized by coupling acetaldehyde with [1,3-$^{13}C_2$]malonic acid using the reaction conditions described above. Briefly, 1.0 mL (18 mmol) of acetaldehyde was added to a solution of [1,3-$^{13}C_2$]-malonic acid (169 mg, 1.6 mmol) in dry pyridine (1.5 mL), and the mixture kept in an ice−water bath overnight. The reaction mixture was then refluxed at 50 °C for 4 h, 1 mL of water was added, and the solution was acidified with concentrated hydrochloric acid to pH 1.5. Extraction with diethyl ether and purification by flash column chromatography yielded 79 mg (0.9 mmol, 56%) of [1-^{13}C]crotonic acid. Subsequently, [1-^{13}C]crotonic acid was converted to the acid chloride by reaction with oxalyl chloride in 90 min and reduced to [1-^{13}C]crotonaldehyde by adding 1.2 equiv of tri-*n*-butyltin hydride in about 1 h using tetrakis(triphenylphosphine)palladium(0) as catalyst (*22*). The reduction of [1-^{13}C]crotonyl chloride was monitored by following the ^{1}H NMR integrals of the crotonyl chloride and crotonaldehyde methyl protons. The resulting aldehyde was isolated by distillation from 70 to 120 °C (0.4 mmHg) and subsequently coupled with malonic acid to produce [3-^{13}C]-hexadienoic acid. The reaction mixture was acidified and extracted with diethyl ether, and the raw product was loaded on a silica gel flash column (2 × 18 cm) and eluted with hexanes:ethyl acetate (4:1). The pure [3-^{13}C]hexadienoic acid was then activated and coupled with CoA as described above. ^{1}H NMR chemical shifts and coupling constants were identical to those observed for unlabeled HD-CoA, except that the multiplet at 7.14 ppm, assigned to the proton attached to the hexadienoyl C3 carbon, was split into a doublet of doublets at 7.01 and 7.27 ppm ($^1J_{H-C}$ = 156 Hz). The ^{13}C NMR spectrum was identical to that of the unlabeled HD-CoA, except that the peak at 146.74 ppm was greatly increased in intensity, consistent with ^{13}C labeling at C3.

4-^{13}C-HD-CoA. Hexadienoyl-CoA labeled with ^{13}C in the hexadienoyl C4 position (4-^{13}C-HD-CoA) was synthesized as described for 3-^{13}C-HD-CoA except that [2-$^{13}C_2$]malonic acid was used. ^{1}H NMR chemical shifts and coupling constants were identical to those observed for unlabeled HD-CoA, except that the multiplet at 6.18 ppm, assigned to the proton attached to the hexadienoyl C4 carbon, was split into a doublet of doublets at 6.05 and 6.31 ppm ($^1J_{H-C}$ = 156 Hz). The ^{13}C NMR spectrum was identical to that of the unlabeled HD-CoA, except that the peak at 131.98 ppm was greatly increased in intensity, consistent with ^{13}C labeling at C4.

5-^{13}C-HD-CoA. Hexadienoyl-CoA labeled with ^{13}C in the hexadienoyl C5 position (5-^{13}C-HD-CoA) was synthesized using the same procedure as that described for 4-^{13}C-HD-CoA except that [1-^{13}C]acetaldehyde and unlabeled malonic acid were used in the first coupling reaction. Specifically, 7.0 mL (21.7 mmol) of tri-*n*-butyltin hydride was added dropwise over a 2 h period to 1.0 g (12.58 mmol) of [1-^{13}C]-acetyl chloride (bp 51 °C) dissolved in 5 mL of dry diethyl ether. The reduction was performed at room temperature using 150 mg (0.14 mmol) of tetrakis(triphenylphosphine)-palladium(0) as the catalyst. To avoid exposure of the resulting aldehyde to air, the [1-^{13}C]acetaldehyde was distilled directly through a connecting tube into a second flask which contained a solution of 3 g of malonic acid in 8 mL of pyridine. After overnight reaction at room temperature, the second flask was refluxed at 50 °C while the first flask was heated to 60 °C for 4 h. Finally, 1 mL of H_2O was added to the reaction mixture and the pH adjusted to 2.0 using concentrated hydrochloric acid. The [3-^{13}C]crotonic acid was extracted with 20 × 10 mL of diethyl ether and purified with a flash column using a 4:1 ratio of hexanes:ethyl acetate. Evaporation in vacuo gave 250 mg of product.

The above [3-^{13}C]crotonic acid (192 mg, 2.2 mmol) was dissolved in 3 mL of dry diethyl ether and converted to the acid chloride using 0.26 mL (3.0 mmol) of oxalyl chloride. The [3-^{13}C]crotonyl chloride was then reduced with 2 mL of tri-*n*-butyltin hydride and introduced, without purification, into a solution of malonic acid (4 g, 38 mmol) in dry pyridine (6 mL) that had been heated to 80 °C. The reaction was kept at 110 °C overnight and cooled to room temperature, and 1 mL of water added. Following acidification to pH 2.0, the 5-^{13}C-HD acid was extracted with 20 × 10 mL of methylene chloride and purified by flash column chromatography (hexanes:ethyl acetate, 4:1). ^{1}H NMR chemical shifts and coupling constants were identical to those observed for unlabeled HD-CoA, except that the multiplet at 6.32 ppm, assigned to the proton attached to the hexadienoyl C5 carbon, was split into two multiplets at 6.19 and 6.45 ppm ($^1J_{H-C}$ = 156 Hz). The ^{13}C NMR spectrum was identical to that of the unlabeled HD-CoA, except that the peak at 127.81 ppm was greatly increased in intensity, consistent with ^{13}C labeling at C5.

Preparation and Purification of Wild-Type and Mutant Enoyl-CoA Hydratases. Recombinant wild-type rat mitochondrial enoyl-CoA hydratase was expressed and purified from cultures of *Escherichia coli* as described (*4*, *7*). The G141P mutant was constructed using QuikChange mutagenesis (Stratagene) (*23*). The mutant plasmid was purified using standard methods, sequenced using dideoxynucleotide methodology (CircumVent thermal cycle dideoxy DNA sequencing kit) and transformed into BL21(DE3)pLysS cells (Novagen) for protein expression.

Determination of Kinetic Parameters and Binding Constants. Kinetic parameters for the reaction of 3′-dephosphocrotonyl-CoA (dpCr-CoA) with G141P were determined in 20 mM phosphate buffer at 25 °C, as described (*4*). The affinity of HD-CoA for enoyl-CoA hydratase was determined at 25 °C in 20 mM phosphate buffer containing 500 mM NaCl using the active site titrant 4-(dimethylamino)cinnamoyl-CoA (DAC-CoA). Previously, it has been shown that the binding of DAC-CoA to the enzyme results in a 96 nm red shift (400 to 496 nm) in the λ_{max} for the (dimethylamino)-cinnamoyl chromophore. Consequently, K_d for the binding of DAC-CoA to the enzyme was determined by absorbance spectroscopy in the presence of varying concentrations of HD-CoA. The dependence of the observed K_d for DAC-CoA with [HD-CoA] was used to determine the K_d for HD-CoA. Initial studies with G141P revealed that the λ_{max} for DAC-CoA did not change on binding to this mutant. Consequently, we used isothermal titration calorimetry (ITC) to determine K_d for the interaction of HD-CoA with G141P. The ITC experiments were performed at 25 °C with 167 μM G141P enzyme in 20 mM sodium phosphate buffer, pH 7.4, containing 500 mM NaCl and 3 mM EDTA. Data were obtained using a MicroCal ITC instrument and analyzed using the MicroCal software (*24*).

Raman Spectroscopy. Raman spectra were acquired using an instrument that has been described in detail elsewhere (*25*). The main feature of this instrument is that all the components have been optimized for operation with near-IR excitation at 752 nm to reduce problems associated with large fluorescence backgrounds that can disrupt Raman studies on biological systems. The Raman measurements on the enzyme complexes were made by adding approximately 60 μL of enzyme to a 2 mm by 2 mm rectangular cell and collecting data for 8 min. Subsequently, a small volume of substrate analogue (1 or 2 μL) was added to the enzyme without making any changes to the optical alignment or to the cell position. Difference Raman spectra were then calculated by performing a computer subtraction of the spectra of the enzyme plus substrate minus the enzyme alone. The difference spectra were wavenumber calibrated against cyclohexanone. All spectral manipulations were carried out using Win-IR software, and data acquisition was performed using WinSpec (Princeton Instruments, Trenton, NJ). Under the conditions used for acquiring good quality difference Raman spectra, the resolution of our system was approximately 10 cm^{-1}.

Vibrational Calculations. The ab initio normal mode calculations on hexadienoyl ethyl thiolester were performed on an Indigo II SGI using Gaussian 98 (*26*). This truncated thiolester can safely be used to model the double bond stretching modes of the hexadienoyl group, which are the focus of the current study, as it has been shown that the CoA portion of HD-CoA does not significantly influence this spectral region (*1*). Density functional theory was employed with B3LYP composite exchange-correlation functionals and a 6-31G** basis set. We found that using either DFT calculations with a 3-21G* basis set or Hartree−Fock calculations with a 6-31G** basis set did not reproduce the experimentally observed energy order for the double bond stretching modes. The *z*-matrix for these calculations was initially set up for the *s-cis* conformer. Once the geometry had been optimized, isotopes were introduced and the vibrational frequencies recalculated. For the *s-trans* conformer the optimized *s-cis* geometry was altered by a rotation of 180° around the C1−O1 bond, the geometry was reoptimized, and vibrational frequencies were calculated. No imaginary frequencies were generated in any of the calculations, suggesting that the global minimum energy was found in each case. When calculated vibrational frequencies are compared with experimentally observed values, a scaling factor is generally introduced to provide closer agreement (*27*). For these calculations we have applied a scaling factor of 0.958.

RESULTS

Raman Band Assignments for the HD-CoA Hexadienoyl Group in Solution. The initial step in interpreting the Raman data for HD-CoA bound to wild-type and mutant enoyl-CoA hydratases is to analyze the Raman data for HD-CoA free in solution. Four single bonds are present in the hexadienoyl portion of HD-CoA, (C3−C4, C1−C2, C1−S, and S−CH_2), rotation about which will result in different conformations of the hexadienoyl group (Figure 2). As rotation about the single bonds can potentially alter the vibrational coupling in the hexadienoyl group, hence affecting the position and intensities of the Raman bands associated with each conformer, it is important to identify the major conformers present in solution and assign their Raman spectra.

Previous NMR studies have shown that the hexadienoyl portion of HD-CoA adopts an *s-trans* conformation about the C3−C4 single bond in solution (*7*). In addition, the thiolester linkage is expected to exist exclusively in a conformation in which the CoA 9″ methylene group and the thiolester carbonyl oxygen are cis to each other (*28*). An additional degree of freedom exists around the S−CH_2 (9″) bond which can adopt either an anti or a gauche conformation. Normal mode calculations on *S*-ethyl thiocrotonate have shown that the conformation of this bond does not have a strong effect on the vibrational spectrum in the spectral regions studied here (*28*). However, two conformations arising from rotation about the C1−C2 single bond are both significantly populated in solution at room temperature and are known to have an effect on the vibrational spectra of enones (*29*). Consequently, the hexadienoyl portion of HD-CoA adopts two major conformations in solution that can significantly influence the vibrational spectrum, in which the C2═C3 ethylenic bond and the C═O group are *cis* (*s-cis*) or *trans* (*s-trans*) to each other (Figure 2).

In the double bond stretching region (1500−1700 cm^{-1}) we expect to find bands attributable to both the *s-cis* and *s-trans* hexadienoyl conformers. This spectral region is dominated by intense bands assigned to the hexadienoyl group, as only very weak bands are present due to the CoA portion of the molecule (*1*). For unlabeled HD-CoA in pH 7.4 phosphate buffer, two intense bands are resolved at 1637 and 1595 cm^{-1}, and a shoulder appears at 1630 cm^{-1} (Figure 3a). These bands are assigned to normal modes involving large contributions from the two C═C stretches in the conjugated hexadienoyl group, since bands attributable to the carbonyl group are usually weak in the Raman spectrum. However, vibrational coupling of the carbonyl group with the two C═C stretches does exert a strong influence on the C═C stretching modes. The exact nature of this coupling is dependent on the conformation around the C1−C2 single bond that links the carbonyl and C═C bonds.

Raman Spectra of Isotopically Labeled HD-CoAs in Solution. In Figure 3 we compare the effect of isotopic labeling on the HD-CoA Raman spectrum. The key data are summarized in Table 1. Although changes in the relative intensities of some of the bands are observed upon labeling, we can assign the major bands in the unlabeled Raman spectrum of HD-CoA as follows. It is known that at low temperature the conformational equilibrium in the model compound hexadienoyl ethyl thiolester shifts in favor of the *s-cis* conformation (*1*). Raman spectra of this model compound as a function of temperature revealed that a band at 1637 cm^{-1} decreased in intensity whereas bands at 1630 and 1595 cm^{-1} increased as the temperature was lowered and the population of the *s-cis* conformer increased. On this basis the two most intense bands at 1637 and 1595 cm^{-1} in HD-CoA are attributed predominantly to C═C stretching modes (coupled to the carbonyl group) for the *s-trans* and *s-cis* conformers, respectively. The band at 1637 cm^{-1} experiences wavenumber shifts on ^{13}C labeling of either of the C═C double bonds and on ^{18}O labeling of the carbonyl group. The isotope shifts are largest for labeling in the terminal (C4═C5) double bond, revealing that this stretching coordinate makes the strongest contribution to this band. In

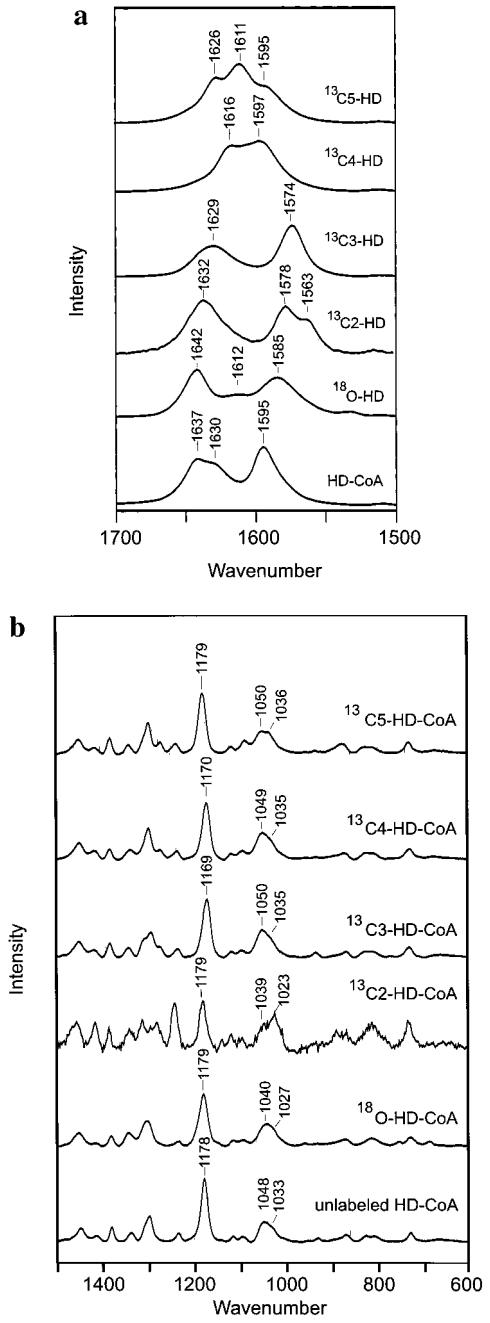

FIGURE 3: Raman difference spectra of HD-CoA and its isotopically labeled analogues in phosphate buffer (pH 7.4, 50 mM, and 500 mM KCl). Data are shown for the (a) 1500−1700 cm^{-1} and (b) 600−1500 cm^{-1} spectral regions. Concentrations of HD-CoAs were between 5 and 20 mM. The data were acquired in 1 min using 752 nm excitation. Solvent bands have been subtracted.

contrast, the band at 1595 cm^{-1} exhibits a strong shift on ^{13}C2 or ^{13}C3 labeling, a smaller shift on ^{18}O labeling, but almost no change on ^{13}C4 or ^{13}C5 labeling. This indicates that the normal mode associated with the 1595 cm^{-1} band has a large contribution from the central (C2═C3) double bond, a weaker contribution from the carbonyl stretch, and little or no contribution from the terminal (C4═C5) double bond. For both major bands coupling with the carbonyl group accounts for the sensitivity to rotation around the C1−C2 single bond. This coupling means that a total of four C═C stretching bands can be expected, two for each conformer. Comparison with the low-temperature spectrum of hexadienoyl ethyl thiolester, which has an increased *s-cis* conformer population and a band maximum near 1630 cm^{-1}, leads to the assignment of the shoulder at 1630 cm^{-1} to a normal mode with a similar composition to the 1637 cm^{-1} band but assigned to the *s-cis* conformer. The fourth C═C stretching band, with a similar composition to the 1595 cm^{-1} band but attributed to the *s-trans* conformer, is not resolved in our data. We also note that the relative intensity of the bands can be influenced by isotope labeling so that in the case of ^{18}O-, ^{13}C2- and ^{13}C5-labeled HD-CoA's the additional bands, due to the mixture of conformers, are much more prominent (Figure 3a).

Table 1: Position of Raman Bands in the Double Bond Stretching Region of Labeled and Unlabeled HD-CoA Free and Bound to Enoyl-CoA Hydratase

	double bond region		single bond region		
		Free HD-CoA			
unlabeled	1637	1595	1178	1048	1033
^{18}O1	1642	1585	1179	1040	1027
^{13}C2	1632	1578	1179	1039	1023
^{13}C3	1629	1574	1169	1050	1035
^{13}C4	1616	1597	1170	1049	1035
^{13}C5	1626	1595	1179	1050	1036
		Bound HD-CoA			
unlabeled	1641	1564	1183	1056	1033
^{18}O1	1641	1549	1184	1053	1038
^{13}C2	1640	1553	1184	1052	1034
^{13}C3	1636	1553	1173	1059	1035
^{13}C4	1627	1565	1174	1060	1032
^{13}C5	1634	1567	1185	1060	1033

It can be expected that other regions of the vibrational spectrum will also be sensitive to the conformational state of the hexadienoyl group. In particular, marker bands can be identified in the C−C single bond stretching region, between about 1000 and 1200 cm^{-1}. From the isotopically labeled data (Figure 3b), the band at 1178 cm^{-1} can be predominantly attributed to the C3−C4 single bond stretching motion. This assignment is based on the fact that the 1178 cm^{-1} band exhibits wavenumber shifts of about 9 cm^{-1} on labeling of the C3 and C4 positions but is insensitive to labels introduced at other positions (Table 1). In contrast, two bands near 1048 and 1033 cm^{-1} are shifted to 1040 and 1027 cm^{-1} and 1039 and 1023 cm^{-1} only for ^{18}O- or ^{13}C2-labeled HD-CoA, respectively, and can be predominantly attributed to C1−C2 single bond stretch coupled to bending motions involving the carbonyl group. The observed isotope shifts are somewhat smaller than the theoretical value for a diatomic oscillator (23 cm^{-1} shift for an isolated C−C stretching band at 1178 cm^{-1}), indicating that there is significant coupling of these motions with other vibrational coordinates.

To test our vibrational assignments for HD-CoA in solution, we have performed ab initio DFT calculations on the *s-cis* and *s-trans* conformers of the model compound hexadienoyl ethyl thiolester and its isotopically labeled analogues. The results of these calculations for the double bond stretching region (1500−1700 cm^{-1}) are listed in Table 2. As the focus of the current study are the bands in the 1500−1700 cm^{-1} region and since we have not included CoA in the calculations, we do not consider the normal modes below 1500 cm^{-1}.

The normal mode calculations correctly predict the energy order of the double bond stretching modes, and after scaling

Table 2: Results of Vibrational Calculations for Bands in the Double Bond Stretching Region for Hexadienoyl Ethyl Thiolester

	C1═O1[a]	C4═C5 and C1═O1[a]	C2═C3[a]
		s-cis Conformer	
unlabeled	1681	1633	1592
^{18}O1	1657	1626	1589
^{13}C1	1654	1624	1587
^{13}C2	1679	1633	1568
^{13}C3	1678	1632	1567
^{13}C4	1679	1609	1592
^{13}C5	1678	1612	1586
		s-trans Conformer	
unlabeled	1669	1640	1602
^{18}O1	1645	1633	1597
^{13}C1	1644	1627	1600
^{13}C2	1668	1638	1579
^{13}C3	1669	1636	1577
^{13}C4	1668	1619	1598
^{13}C5	1668	1625	1590

[a] Isotope labeling of the atoms in these double bonds is calculated to produce significant wavenumber shifts in the Raman spectrum.

the values are reasonably close to those experimentally observed (Table 1). All three double bonds are involved at some level in each normal mode, but only those bonds which produce significant changes on isotope labeling are listed (Table 2). On the basis of these calculations we find that the carbonyl stretching modes are predicted to appear at 1681 and 1669 cm^{-1} for the *s-cis* and *s-trans* conformers, respectively. These bands are presumably too weak to be observed in the experimental Raman spectra. However, the two predominantly C═C stretching bands are calculated at 1633 and 1592 cm^{-1} for the *s-cis* conformer and 1640 and 1602 cm^{-1} for the *s-trans* conformer, closely matching the experimental values. The higher wavenumber band involves mainly the C4═C5 and C1═O1 bonds. In contrast, the main contribution to the lower wavenumber band is from the C2═C3 double bond. These calculations also reflect the fairly small wavenumber differences between the two conformers for free HD-CoA. The only discrepancy between calculation and experiment is that the calculations do not correctly predict the wavenumber shifts in the 1637 cm^{-1} band observed for ^{13}C2- and ^{13}C3-labeled HD-CoA. According to the calculations there is no change in the frequency of this band for these particular labels. However, the experimental data reveal that shifts of around 10 cm^{-1} occur upon labeling (Figure 3a). This indicates that the band at 1637 cm^{-1} actually has some significant C2═C3 character in free HD-CoA.

Raman Band Assignments for HD-CoA Bound to Wild-Type Enoyl-CoA Hydratase. The difference Raman spectra of HD-CoA and its isotopically labeled analogues bound to wild-type enoyl-CoA hydratase are presented in Figure 4. The two bands observed at 1637 and 1630 cm^{-1} in the spectrum of free HD-CoA (Figure 3a) are replaced by an intense band at 1641 cm^{-1} (Figure 4). In addition, the band at 1595 cm^{-1} in the free spectrum shifts to 1564 cm^{-1} and approximately doubles in intensity relative to the higher wavenumber band upon binding (Figure 4). By comparison with earlier studies, the 1641 and 1564 cm^{-1} bands are assigned to HD-CoA bound in a *s-cis* conformation. Thus, the 1630 cm^{-1} band assigned to the *s-cis* conformer in free HD-CoA shifts to higher wavenumber upon binding whereas the 1595 cm^{-1} shifts to lower wavenumber. In addition, the

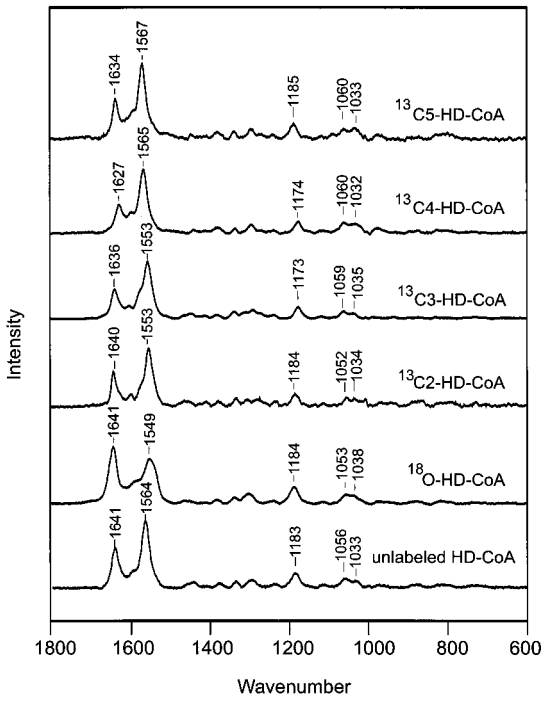

FIGURE 4: Raman difference spectra between 600 and 1800 cm^{-1} of HD-CoA and its isotopically labeled analogues bound to wild-type enoyl-CoA hydratase in 50 mM phosphate buffer, pH 7.4, and 500 mM KCl. In each case 0.8 equiv of HD-CoA was added to 800 μM enzyme, and the data were acquired in 8 min.

isotope labeling indicates that the 1641 cm^{-1} band is only sensitive to labeling of the terminal (C4═C5) double bond and that the band at 1564 cm^{-1} involves only the enone (C3═C2−C1═O1) group. These data are in agreement with the earlier difference Raman study (*1*) and provide the *first* direct evidence for the assignment of the band at 1641 cm^{-1}. These observations can only be explained if the enzyme's active site is causing a significant redistribution in the normal modes on binding, which results in the intense Raman band at 1564 cm^{-1} being generated exclusively by the enone fragment (C3═C2−C1═O1) of HD-CoA and the intense band at 1641 cm^{-1} by the terminal double bond in isolation.

In the single bond stretching region the isotope-labeled spectra of HD-CoA bound to wild-type enzyme are similar to the data on HD-CoA free in solution. In particular, the band which appears at 1183 cm^{-1} in the bound spectrum is only sensitive to ^{13}C3 and ^{13}C4 labeling, identifying it as predominantly involving the C3−C4 stretching motion. In addition, two bands appear at 1056 and 1033 cm^{-1} in the spectrum of unlabeled HD-CoA bound to wild-type enzyme. These bands probably correspond to the two bands observed at 1048 and 1033 cm^{-1} for HD-CoA free in aqueous solution (Figure 3b). However, the separation between the two bands has increased, leading to a better definition of the two peaks.

G141P Kinetic Parameters and Binding Constants. G141P was expressed with an N-terminal His-tag, which was subsequently removed following purification. The mutant enzyme bound to the CoA affinity column and eluted at the same salt concentration as wild type, suggesting that the mutation had not disrupted the CoA binding pocket. Table 3 compares the k_{cat}, K_m, and K_d values for the wild-type and G141P enzymes. Replacement of G141 with proline does not affect the K_m for dpCr-CoA but results in a (1.4×10^6)-fold reduction in k_{cat}. In addition, the K_d for HD-CoA

Table 3: Kinetic Parameters and Dissociation Constants for Wild-type and G141P enoyl-CoA hydratase

enzyme	k_{cat} (s^{-1})[a]	K_m (μM)[a]	k_{cat}/K_m (μM^{-1} s^{-1})[a]	K_d (μM)[b]
wild type	1380 ± 50	89 ± 9	15.5 ± 2.1	105 ± 8.0
G141P	0.00101 ± 0.00004	105 ± 10	0.0000096 ± 1.1	23 ± 0.7

[a] Kinetic parameters for the hydration of 3′-dephosphocrotonyl-CoA were determined at 25 °C in 20 mM pH 7.4 sodium phosphate buffer containing 3 mM EDTA. Data for the wild-type enzyme were taken from Hofstein et al. (*41*). [b] Dissociation constants for HD-CoA binding to enoyl-CoA hydratase were determined at 25 °C in 20 mM pH 7.4 sodium phosphate buffer containing 500 mM NaCl and 3 mM EDTA. K_d for the wild-type enzyme was determined using the DAC-CoA titration method while K_d for G141P was determined using isothermal titration calorimetry.

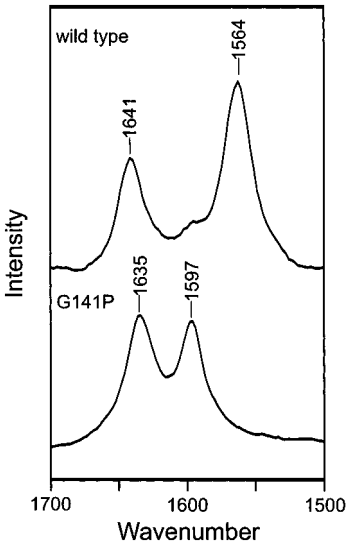

FIGURE 5: Raman difference spectra between 1500 and 1700 cm^{-1} of unlabeled HD-CoA bound to wild-type enoyl-CoA hydratase and the G141P mutant in 50 mM phosphate buffer, pH 7.4, and 500 mM KCl. For both experiments 0.8 equiv of HD-CoA was added to 800 μM enzyme, and the data were acquired in 8 min.

determined using ITC was 23 ± 1 μM for G141P, lower than the K_d of 105 ± 8 μM and 150 ± 4 μM observed for wild-type enzyme using the DAC-CoA binding assay and ITC, respectively. Taken together, these data strongly suggest that the glycine to proline substitution has not significantly perturbed the overall protein conformation or the substrate binding site and that changes in enzyme activity and Raman spectra in the G141P enzyme can be ascribed mainly to the removal of a specific hydrogen bond between the enzyme and ligand.

Raman Spectroscopy. The difference Raman spectrum of HD-CoA bound to the G141P mutant between 1500 and 1700 cm^{-1} is displayed in Figure 5 where it is compared with the Raman spectrum of HD-CoA bound to wild-type enzyme. The main difference between the Raman spectra of HD-CoA bound to the two enzymes is that the 1564 cm^{-1} band observed in the wild-type spectrum and assigned to a normal mode involving the hexadienoyl C3═C2−C1═O1 enone fragment has been replaced by a band at 1597 cm^{-1} in the G141P spectrum. From these data we conclude that the hexadienoyl group is no longer polarized by the enzyme. Indeed, the Raman spectrum of HD-CoA bound to G141P is similar to the free HD-CoA spectrum (Figure 3a). Under the conditions of the Raman experiment with 800 μM G141P and 640 μM HD-CoA, we calculate, using a K_d of 23 μM, that 91% of HD-CoA is bound to the G141P enzyme.

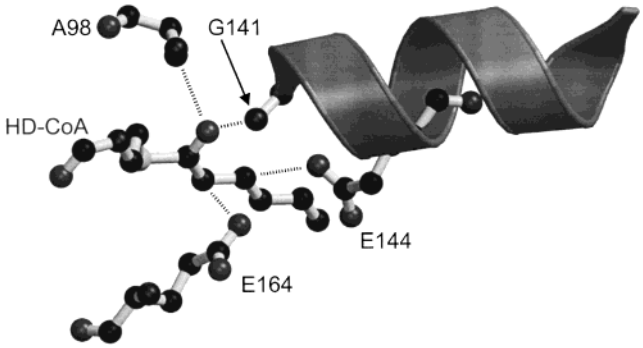

FIGURE 6: HD-CoA modeled into the active site of enoyl-CoA hydratase in an *s-cis* conformation. The modeling was performed using the X-ray structure of enoyl-CoA hydratase complexed with octanoyl-CoA (*10*) with Insight II (Biosym, MSI).

DISCUSSION

The isotope-labeled Raman spectra (Figure 4) provide direct evidence for the complete decoupling of the terminal double bond and the enone fragment of the hexadienoyl group in HD-CoA upon binding to wild-type enoyl-CoA hydratase in an *s-cis* conformation (Table 1). This observation highlights the considerable polarizing force being exerted on the ground state of the substrate analogue by the enzyme's active site. A number of structural features around the enzyme's active site may potentially be contributing to the observed polarization (Figure 6). In particular, two hydrogen bonds between the amide backbone of residues A98 and G141 have been identified in the crystal structures of enoyl-CoA hydratase in complex with acetoacetyl-CoA (*9*) and octanoyl-CoA (*10*). In addition, the G141 residue is located at the end of an α-helix that points toward the active site, so the helix dipole may be increasing the strength of the hydrogen bond between the G141 amide hydrogen and the hexadienoyl carbonyl group (*30*−*32*). These interactions will also be of primary importance for stabilizing the transition state for the enzyme-catalyzed reaction when negative charge will accumulate on the carbonyl oxygen.

To investigate the importance of the interactions depicted in Figure 6 on polarization and reactivity, we have begun to replace amino acids in the active site and monitor the effect using kinetics and Raman spectroscopy. Replacement of G141 with a proline results in an approximately 10^6-fold decrease in k_{cat} while leaving K_m unaffected. Interestingly, a similar decrease in reactivity has been observed in acyl-CoA dehydrogenase where the specific removal of a hydrogen bond to the substrate carbonyl resulted in an approximately 10^7-fold decrease in the rate of substrate oxidation (*33*). The fact that the G141P enoyl-CoA hydratase mutant binds to the CoA affinity column with an affinity similar to that of wild-type enzyme and that the K_d for the binding of HD-CoA is actually lower in the mutant compared to wild type provides strong evidence that the mutation has not resulted in a major alteration in the structure of the active site. Furthermore, we note that the Ramachandran angles of G141, which are ϕ −54°, ψ −31° (*9*, *10*), are compatible with substitution by a proline [preferred ϕ −60° (*18*)].

In addition to the changes in reactivity, removal of the G141 hydrogen bond completely abolishes the ability of the

enzyme to polarize the ground state of HD-CoA, suggesting a direct link between polarization and reactivity. Since substituting glycine with proline must remove the hydrogen bond between the substrate and residue 141, the observed loss of polarization and decrease in activity could in principle result simply from loss of this hydrogen-bonding interaction. If this is so, then the hydrogen bond between G141 and the substrate would have to be worth 34 kJ/mol in the transition state, since this is how much the activation energy for the reaction increases based on a 10^6-fold decrease in k_{cat}/K_m. Furthermore, since the hydrogen bond will strengthen in the transition state, as charge is redistributed, the ground-state hydrogen bond enthalpy will likely be less than 34 kJ/mol. While the present Raman data do not provide specific information on the energetics of the interaction between the HD-CoA carbonyl and the enzyme in the ground state, it is noteworthy that in a previous resonance Raman study we observed that removal of a single hydrogen bond in the oxyanion hole of subtilisin resulted in a 32 cm^{-1} increase in $\nu_{C=O}$ for an α,β-unsaturated acyl-enzyme and estimated that the effective hydrogen bond enthalpy required to change $\nu_{C=O}$ by this amount was 32 kJ/mol (*34*, *35*). Indeed, hydrogen bond strengths of around 30 kJ/mol or greater have been estimated in enzyme active sites (*36*, *37*). Consequently, it is possible that the hydrogen bond from G141 may supply sufficient energy to account for the observed decrease in k_{cat}.

A further possibility is that the position of the substrate with respect to catalytic residues in the active site, such as E144 and E164, has been altered either as a result of removing the G141−ligand hydrogen bond and/or because replacement of G141 with proline has perturbed the active site architecture. While there is evidence that the overall structure of the active site has not been substantially perturbed, we shall have to wait for data from X-ray crystallographic studies to address the impact of mutagenesis on the active site structure. We also note that replacement of E164, one of the catalytic glutamates, with aspartate results in a 10^3-fold reduction in k_{cat} (unpublished data). In this mutation the distance between the catalytic group and the substrate has presumably increased, suggesting that repositioning of the substrate with respect to this amino acid in the G141P enzyme could impact reactivity.

On the basis of the results from our extensive isotope labeling experiments and the vibrational calculations on the free and bound ligand, we can propose a physical explanation for the observed ground-state polarization of HD-CoA. On binding to the enzyme two intense bands assigned to the *s-cis* conformer are altered. The band at 1595 cm^{-1} shifts to 1564 cm^{-1}, and for both free and bound HD-CoA, this particular band is only sensitive to isotopic labeling in the enone portion of the hexadienoyl group. The large shift to lower wavenumber of this enone band provides strong evidence that both the carbonyl and C2═C3 bonds are losing double bond character on binding to the enzyme. This wavenumber shift is not observed for the G141P/HD-CoA complex, implicating the G141−ligand hydrogen bond as the important determinant for polarization. In contrast, the other *s-cis* conformer band, observed at 1630 cm^{-1} in free HD-CoA, shifts to higher wavenumber on binding (1641 cm^{-1}) and is only sensitive to labeling in the terminal C4═C5 double bond. These two observations are consistent with a strengthening of this double bond on binding to the enzyme. Thus, the conjugated hexadienoyl group has become selectively polarized, which activates the C2═C3 bond for the hydration chemistry. One reasonable explanation for this decoupling would be a twist around the C3−C4 bond leading to a loss of conjugation in the hexadienoyl group. However, an earlier transferred NOE NMR study found no evidence for a loss of planarity in HD-CoA on binding to enoyl-CoA hydratase (*7*). Consequently, we postulate that the uncoupling results from the specific alignment of the hexadienoyl group with the local electric field in the active site (*5*).

Finally, Raman spectroscopy has also been used to study the structure of ligands bound to 4-chlorobenzoyl-CoA dehalogenase, a second member of the hydratase superfamily (*38*−*40*). The large changes in the electronic structure of ligands bound to the dehalogenase have been ascribed in part to a "pull" of electron density from the oxyanion hole and accompanying α-helix. As noted by Gerlt and co-workers (*11*, *14*), stabilization of negative charge on the substrate carbonyl is likely a common theme in reactions catalyzed by members of the hydratase superfamily. Here we present the first direct evidence for the importance of G141 in substrate polarization and reactivity in enoyl-CoA hydratase.

REFERENCES

1. Tonge, P. J., Anderson, V. E., Fausto, R., Kim, M., Pusztai-Carey, M., and Carey, P. R. (1995) *Biospectroscopy 1*, 387−394.
2. Willadsen, P., and Eggerer, H. (1975) *Eur. J. Biochem. 54*, 247−252.
3. Furuta, S., Miyazawa, S., Osumi, T., Hashimoto, T., and Ui, N. (1980) *J. Biochem. 88*, 1059−1070.
4. Hofstein, H. S., Feng, Y., Anderson, V. E., and Tonge, P. J. (1999) *Biochemistry 38*, 9508−9516.
5. D'Ordine, R. L., Tonge, P. J., Carey, P. R., and Anderson, V. E. (1994) *Biochemistry 33*, 12635−12643.
6. D'Ordine, R. L., Tonge, P. J., Carey, P. R., and Anderson, V. E. (1994) *Biochemistry 33*, 12635−12643.
7. Wu, W. J., Anderson, V. E., Raleigh, D. P., and Tonge, P. J. (1997) *Biochemistry 36*, 2211−2220.
8. Kiema, T. R., Engel, C. K., Schmitz, W., Filppula, S. A., Wierenga, R. K., and Hiltunen, J. K. (1999) *Biochemistry 38*, 2991−2999.
9. Engel, C. K., Mathieu, M., Zeelen, J. P., Hiltunen, J. K., and Wierenga, R. K. (1996) *EMBO J. 15*, 5135−5145.
10. Engel, C. K., Kiema, T. R., Hiltunen, J. K., and Wierenga, R. K. (1998) *J. Mol. Biol. 275*, 847−859.
11. Haller, T., Buckel, T., Retey, J., and Gerlt, J. A. (2000) *Biochemistry 39*, 4622−4629.
12. Benning, M. M., Taylor, K. L., Liu, R.-Q., Yang, G., Xiang, H., Wesenberg, G., Dunaway-Mariano, D., and Holden, H. M. (1996) *Biochemistry 35*, 8103−8109.
13. Modis, Y., Filppula, S. A., Novikov, D. K., Norledge, B., Hiltunen, J. K., and Wierenga, R. K. (1998) *Structure 6*, 957−970.
14. Benning, M. M., Haller, T., Gerlt, J. A., and Holden, H. M. (2000) *Biochemistry 39*, 4630−4639.
15. Benning, M. M., Taylor, K. L., Liu, R.-Q., Yang, G., Xiang, H., Wesenberg, G., Dunaway-Mariano, D., and Holden, H. M. (1996) *Biochemistry 35*, 8103−8109.
16. Clarkson, J., Tonge, P. J., Taylor, K. L., Dunaway-Mariano, D., and Carey, P. R. (1997) *Biochemistry 36*, 10192−10199.
17. Taylor, K. L., Xiang, H., Liu, R. Q., Yang, G., and Dunaway-Mariano, D. (1997) *Biochemistry 36*, 1349−1361.
18. Ramachandran, G. N., and Sasisekharan, V. (1968) *Adv. Protein Chem. 23*, 283−438.
19. Richardson, J. S., and Richardson, D. C. (1988) *Science 240*, 1648−1652.
20. Ellman, G. L. (1959) *Arch. Biochem. Biophys. 82*, 70−77.

21. Koo, J., Fish, M. S., Walker, G. N., and Blake, J. (1963) in *Organic Synthesis*, pp 327−328, Wiley, New York.
22. Four, P., and Guibe, F. (1981) *J. Org. Chem. 46*, 4439−4445.
23. Parikh, S., Moynihan, D. P., Xiao, G., and Tonge, P. J. (1999) *Biochemistry 38*, 13623−13634.
24. Bhatnagar, R. S., and Gordon, J. I. (1995) *Methods Enzymol. 250*, 467−486.
25. Rudik, I., Bell, A. F., Tonge, P. J., and Thorpe, C. (2000) *Biochemistry 39*, 92−101.
26. Frisch, M. J., Trucks, G. W., Schlegel, H. B., Scuseria, G. E., Robb, M. A., Cheeseman, J. R., Zakrzewski, V. G., Montgomery, J. A., Jr., Stratmann, R. E., Burant, J. C., Dapprich, S., Millam, J. M., Daniels, A. D., Kudin, K. N., Strain, M. C., Farkas, O., Tomasi, J., Barone, V., Cossi, M., Cammi, R., Mennucci, B., Pomelli, C., Adamo, C., Clifford, S., Ochterski, J., Petersson, G. A., Ayala, P. Y., Cui, Q., Morokuma, K., Malick, D. K., Rabuck, A. D., Raghavachari, K., Foresman, J. B., Cioslowski, J., Ortiz, J. V., Stefanov, B. B., Liu, G., Liashenko, A., Piskorz, P., Komaromi, I., Gomperts, R., Martin, R. L., Fox, D. J., Keith, T., Al-Laham, M. A., Peng, C. Y., Nanayakkara, A., Gonzalez, C., Challacombe, M., Gill, P. M. W., Johnson, B. G., Chen, W., Wong, M. W., Andres, J. L., Head-Gordon, M., Replogle, E. S., and Pople, J. A. (1998) *Gaussian 98*, Gaussian, Inc., Pittsburgh, PA.
27. Wong, M. W., Wiberg, K. B., and Frisch, M. J. (1991) *J. Chem. Phys. 95*, 8991−8998.
28. Fausto, R., Tonge, P. J., and Carey, P. R. (1994) *J. Chem. Soc., Faraday Trans. 90*, 3491−3503.
29. Gawronski, J. (1989) in *The Chemistry of Enones* (Patai, S., and Rappoport, Z., Eds.) pp 55−105, Wiley, Chichester.
30. Hol, W. G., van Duijnen, P. T., and Berendsen, H. J. (1978) *Nature 273*, 443−446.
31. Lockhart, D. J., and Kim, P. S. (1992) *Science 257*, 947−951.
32. Kortemme, T., and Creighton, T. E. (1995) *J. Mol. Biol. 253*, 799−812.
33. Engst, S., Vock, P., Wang, M., Kim, J. J. P., and Ghisla, S. (1999) *Biochemistry 38*, 257−267.
34. Tonge, P. J., and Carey, P. R. (1992) *Biochemistry 31*, 9122−9125.
35. Tonge, P. J., Fausto, R., and Carey, P. R. (1996) *J. Mol. Struct. 379*, 135−142.
36. Mildvan, A. S., Harris, T. K., and Abeygunawardana, C. (1999) *Methods Enzymol. 308*, 219−245.
37. Shan, S. O., and Herschlag, D. (1999) *Methods Enzymol. 308*, 246−276.
38. Taylor, K. L., Liu, R. Q., Liang, P. H., Price, J., Dunaway-Mariano, D., Tonge, P. J., Clarkson, J., and Carey, P. R. (1995) *Biochemistry 34*, 13881−13888.
39. Clarkson, J., Tonge, P. J., Taylor, K. L., Dunaway-Mariano, D., and Carey, P. R. (1997) *Biochemistry 36*, 10192−10199.
40. Dong, J., Xiang, H., Luo, L., Dunaway-Mariano, D., and Carey, P. R. (1999) *Biochemistry 38*, 4198−4206.
41. Hofstein, H. A., Feng, Y., and Tonge, P. J. (2000) manuscript in preparation.

BI001733Z